Biotechnology and Bioprocess Engineering 28: 125-136 (2023)
DOI 10.1007/s12257-021-0229-4

pISSN 1226-8372
eISSN 1976-3816

RESEARCH PAPER

# Hsa_circ_0001165 Regulates the Malignant Phenotype and Angiogenesis of Prostate Cancer Cells through miR-654-3p/DDAH1

**Shiben Ji, Ci Zhang, Yang Xiang, and Guohong Yin**

Received: 20 August 2021 / Revised: 9 November 2021 / Accepted: 22 November 2021


**Abstract** Prostate cancer (PCa) is one of the most common malignant tumors, with a high rate of metastasis and recurrence. Circular RNA_0001165 (circ_0001165) has been shown to be involved in the advance of PCa. However, the interaction between circ_0001165 and microRNA in PCa has not been studied. Quantitative real-time polymerase chain reaction was used to detect the expression of related genes in PCa tissues and cells. The expression of related epithelial-mesenchymal transition proteins was detected by Western blotting. The interaction of miR-654-3p with circ_0001165 or dimethylarginine dimethylaminohydrolase 1 (DDAH1) has been notarized by Dual-luciferase reporter assay and RNA immunoprecipitation assay. Xenotransplantation experiments confirmed the function of circ_0001165 *in vivo*. Circ_0001165 and DDAH1 are significantly high-expressed in PCa tissues and cells. Silencing circ_0001165 can reduce the proliferation, migration, invasion and tube formation of LNCaP and DU145 cells. MiR-654-3p is a target of circ_0001165. Silencing circ_0001165 can inhibit the malignant behavior of PCa cells by releasing miR-654-3p. In addition, DDAH1 is a target of miR-654-3p. Over-expression of DDAH1 partially restored the inhibitory effect of miR-654-3p on cell proliferation. Animal experiments confirmed the anti-tumor effect of silence circ_0001165 *in vivo*. Circ_0001165 regulates the expression of DDAH1 by regulating miR-654-3p, thereby mediating the process of PCa, and at least partially promoting the development of PCa cells, providing a novel targeted therapy for PCa.

**Keywords:** circ_0001165, miR-654-3p, DDAH1, prostate cancer

Shiben Ji, Yang Xiang, Guohong Yin*
Department of Urology, Wuhan Hankou Hospital, Wuhan, Hubei 430014, China
Tel: +86-13437103305; Fax: +86-27-82876166
E-mail: ghyin1343710@163.com

Ci Zhang
Department of Urology, ZhongNan Hospital of Wuhan University, Wuhan, Hubei 430071, China

## 1. Introduction

Prostate cancer (PCa) is one of the most common cancers threatening the health of men today due to its high morbidity and mortality [1,2]. The incidence of the disease increases with age, and the most common group is elderly men [3,4]. Although the 5-year survival rate of PCa is high and the cure rate is high, the spread of cancer cells in advanced PCa can lead to poor prognosis [5,6]. Therefore, it is still necessary to search for effective PCa biomarkers for early detection.

Circular RNAs (circRNAs), as a covalently closed loop, are members of the non-coding RNA family commonly found in eukaryotic cells [7,8]. In recent years, many researchers have devoted themselves to studying the role of circRNAs in various cancer diseases, including PCa. For example, circ_0057558 [9], circUBAP2 [10], and circPDHX [11] have been studied to play a carcinogenic role in PCa. In addition, Yan *et al.* [12] showed that circ_0001165 can promote the development of PCa by regulating tumor necrosis factor through miR-187-3p. However, the mechanism of action of circ_0078767 in PCa has not been fully studied.

CircRNAs, as competitive endogenous RNAs (ceRNAs), can effectively regulate gene transcription through sponge microRNAs (miRNAs) [13]. Studies have shown that miRNA can interact with mRNA 3'UTR and exert negative regulation [14, 15]. Numerous studies have found that miR-

654-3p plays a role in a variety of cancers. For example, Pu *et al.* [16] showed that miR-654-3p regulates the progression of non-small cell lung cancer by targeting PLK4. Yang *et al*.'s [17] study found that miR-654-3p plays a tumor suppressive role in hepatocellular carcinoma. Similarly, Formosa *et al*. [18] found that miR-654-3p played a carcinogenic role in PCa tissues and cells. However, the mechanism of miR-654-3p in PCa has not been fully understood and is still worth studying.

Dimethylarginine dimethylaminohydrolase 1 (DDAH1), a subtype of the enzyme family that metabolizes methylated arginine, is widely expressed in the kidney, brain, and liver of mammals [19-21]. Studies have shown that DDAH1 plays a role in a variety of cancers, including gastric cancer [22], breast cancer [23], and PCa [24]. However, it is still unclear whether DDAH1 is regulated by circ_0001165 in PCa.

Here, we discovered that circ_0001165 was highly expressed in PCa tissues and cells. Furthermore, we aimed to find that circ_0001165 can regulate PCa through a novel molecular mechanism of miR-654-3p/DDAH1, and come up with a novel idea for the cure of PCa.

## 2. Materials and Methods

### 2.1. Patients and cell lines

Prostate tumor specimens and para-hepatic normal prostate tissue of 48 patients with PCa in Wuhan Hankou Hospital were collected. Each patient offered written informed consent and received supervision and guidance from the Wuhan Hankou Hospital Ethics Committee. None of the samples received any preoperative treatment and were immediately frozen in liquid nitrogen and stored at -80°C until use.

Human normal prostate epithelial cells (RWPE-1), human PCa cell lines (LNCaP and DU145) and HEK293T cells were purchased from American Type Culture Collection (Manassas, VA, USA). These cells were routinely cultured in Dulbecco's modified Eagle medium (DMEM; Invitrogen, Carlsbad, CA, USA) supplemented with 10% fetal bovine serum (FBS; Thermo Fisher Scientific, Rockville, MD, USA) at 37°C in a humidified incubator containing 5% $CO_2$.

### 2.2. Cell transfection

For short hairpin RNA (shRNA) targeting circ_0001165 (sh-circ_0001165#1, sh-circ_0001165#2) and its control group (sh-NC), overexpression of circ_0001165 vector (circ_0001165) and its control group (vector), miR-654-3p inhibitor (anti-miR-654-3p) and its control group (anti-miR-NC), and the DDAH1 overexpression vector (DDAH1) and matching control (pcDNA3.1) were synthesized by RiboBio Ltd. (Guangzhou, China) and then transfected into LNCaP and DU145 cells using Lipofectamine 2000 (Promega, Madison, WI, USA).

### 2.3. Quantitative real-time polymerase chain reaction (qRT-PCR)

After 48 h of LNCaP and DU145 cell transfection, Trizol reagents (Thermo Fisher Scientific) were used to isolate total RNA from PCa tissues or cells. Using reverse transcription kit (Thermo Fisher Scientific) reversed transcripts total RNA to cDNA. qRT-PCR was performed by miScript SYBR Green PCR Kit (Qiagen NV, Venlo, Netherlands). Using GAPDH or U6 as internal reference, and the relative expression level was calculated by $2^{-\Delta\Delta CT}$. Primer sequences was established in Table S1.

### 2.4. Western blot analysis

After 48 h of LNCaP and DU145 cell transfection, radioimmunoprecipitation analysis buffer (Thermo Fisher Scientific) was used to extract the total protein. Then total proteins were quantified by BCA protein assay kit (Pierce, Rockford, IL, USA) and electrophoresis using 12% SDS-PAGE. After transferring the protein to the PVDF membrane, using 5% skim milk blocked the membrane, anti-β-actin (1:1,000, ab8226, Abcam, Cambridge, MA, USA), anti-Snail (1:1,000, ab216347, Abcam), anti-Slug (1:1,000, ab27568, Abcam), and anti-DDAH1 (1:1,000, ab108088, Abcam) were incubated. Last, Clarity™ Western ECL Substrate Kit (Bio-Rad, Shanghai, China) was used to develop bands of proteins.

### 2.5. RNase R degradation and actinomycin D treatment assay

RNase R (3 U/μg; Epicentre Technologies, Madison, WI, USA) was incubated with total RNA (3 μg) at 37°C for 30 min. Transcription was inhibited by adding actinomycin D (2 mg/mL; Sigma-Aldrich, St. Louis, MO, USA) to the LNCaP and DU145 cells culture medium for 4, 8, 12, and 24 h. qRT-PCR was used to measure the corresponding expression level of the treated cells.

### 2.6. 3-(4, 5-dimethylthiazol-2-yl)-2, 5-diphenyltetrazolium Bromide (MTT) assay

Transfected LNCaP and DU145 cells ($1 \times 10^4$ cells per well) were seeded into 96-well plates. Then each well added 20 μL MTT solution (Thermo Fisher Scientific), after incubate 4 h, 200 μL dimethyl sulfoxide (Sigma-Aldrich) were added to dissolve formazan crystal. The absorbance at 570 nm was measured with an enzyme marker (BioTek, Winooski, VT, USA).

### 2.7. Thymidine analog 5-ethynyl-2'-deoxyuridine (EdU) assay

Transfected LNCaP and DU145 cells ($2 \times 10^4$/mL) were seeded in 200 μL DMEM medium containing 10% FBS, then added 50 μM the Cell-Light EdU DNA Cell Proliferation Kit (RiboBio Ltd.) for 24 h and then water bath at 37°C for 2 h. The cells were then stained with Apollo staining solution and Hoechst 33,342 in the kit according to the instructions and observed under a fluorescence microscope (Leica, Wetzlar, Germany).

### 2.8. Colony formation assay

The transfected LNCaP and DU145 cells were seeded into 6-well plates (200 cells/well). After incubation for 2 weeks, the cells were fixed with paraformaldehyde, and then stained with crystal violet. The colonies were observed and counted under a light microscope (Nikon, Tokyo, Japan).

### 2.9. Wound-healing assay

LNCaP and DU145 cells were inoculated into 6-well plates at a density of $5 \times 10^4$ cells/well after 48 h of transfection, and the plates were scratched vertically with a pipette tip after 24 h. Then serum-free medium was added for 24 h. Microscopic photographs were taken to observe the width of the scratches at 0 h and 24 h. Then serum-free medium was added and incubated for 24 h. Microscopic photographs were taken to observe the width of the scratches at 0 h and 24 h.

### 2.10. Transwell assay

The ability of LNCaP and DU145 cells invasion was detected by Transwell. Matrigel (BD Biosciences, San Diego, CA, USA) is covered in Transwell chambers (Corning, Madison, NY, USA), $5 \times 10^4$ cells were added into the upper of Transwell chambers. Meanwhile, the Transwell lower chambers was added with fresh culture medium containing 10% FBS. The amount of invaded cells was counted under a high-powered microscope.

### 2.11. Flow cytometry assay

Transfected SW480 and HCT116 cells were double stained with Annexin V-fluorescein isothiocyanate (FITC)/propidium iodide (PI), processed as recommended by the manufacturers (BD Biosciences). And the cell cycle of the transfected LNCaP and DU145 cells incubated with 1 mL of PI/TritonX-100 staining solution (containing 0.2 mg RNase A, 20 μg of PI, and 0.1% TritonX-100) at 4°C for 30 min. The apoptotic cells and cell cycle were then detected by flow cytometry (BD Biosciences).

### 2.12. Tube formation assay

Matrigel is covered with 48-well plates. After Matrigel curing for 1 h, 200 μL cell suspension was inoculated onto the gel. After incubation for 4-6 h, observation was made under a microscope and photos were taken. The ImageJ software (National Institutes of Health, Bethesda, MD, USA) was used to quantify the tube formation.

### 2.13. RNA immunoprecipitation (RIP) assay

RIP assay was performed using an Imprint RNA immunoprecipitation kit (Sigma-Aldrich). Transfected Huh7 and SNU-387 cells were lysed in RIP lysis buffer. Cell lysate was incubated with human anti-Argonaute2 (anti-Ago2) or negative control magnetic beads coupled with normal anti-IgG for 12 h at 4°C. The relative enrichment of circ_0001165 and miR-654-3p were determined by qRT-PCR analysis.

### 2.14. Immunohistochemical (IHC) staining analysis

Resected tissues were fixed with 4% buffered paraformaldehyde, dehydrated and embedded in paraffin. Paraffin sections (5 μM) were dewaxed and rehydrated for antigen stripping. Then anti-Ki67 (1:2,000, ab15580, Abcam) was placed at 4°C overnight, and matched with the Goat against mouse IgG (1:10,000, ab205719, Abcam) 1 h. Sections were stained with diaminobenzidine kit (Sigma-Aldrich) according to protocol. The positive staining was observed with a light microscope.

### 2.15. Dual-luciferase reporter assay

The sequences of circ_0001165 or DDAH1 3'UTR containing presumed miR-654-3p interacting sites were cloned into pGL3-basic vectors (Realgene, Nanjing, China), respectively. HEK293T cells in 48-well plates ($8 \times 10^3$ cells/well) were transfected with luciferase reporter plasmid in combination with miR-654-3p or control by Lipofectamine 2000 (Promega). The relative luciferase activities were measured by Dual-Luciferase Reporter Assay Kit (GeneCopoeia, Rockville, MD, USA) after transfection 48 h, with Renilla luciferase activity as control.

### 2.16. Animal experiment

Balb/c mice (female, 6 weeks old) were purchased from Beijing Vital River Laboratory Animal Technology Co., Ltd. (Beijing, China). Sh-circ_0001165 DU145 cells were injected into $1.5 \times 10^6$ cells/mice, subcutaneous tumor size was measured every five days. The tumor volume was calculated by the formula: volume = 1/2 (length × width$^2$). On day 30, the mice were euthanized to remove subcutaneous tumors and measure tumor quality. Then the corresponding experiment was carried out. All animal experiments are carried out in accordance with the instructions of Wuhan Hankou Hospital Animal Care and Use Committee (IACUC No.2020HK551).

### 2.17. Statistical analysis

GraphPad Prism 7 (GraphPad Software, San Diego, CA, USA) was utilized for data analysis. Difference comparison between groups were determined using Student's *t*-test or one-way analysis of variance. Each experiment was carried out at least three times and the final data were shown as the mean ± standard deviation. Using $p < 0.05$ meant significant difference.

## 3. Results

### 3.1. Circ_0001165 was up-regulated in PCa tissue and cells

As shown in Fig. 1A was the structure diagram of circ_0001165. A total of 48 PCa patients were enrolled in this study and the expression of circ_0001165 was substantially up-regulated in tumor tissue (Fig. 1B). And comparing to normal RWPE-1 cells, the PCa cell line (LNCaP and DU145) was also significantly increased of circ_0001165 expression (Fig. 1C). Meanwhile, compared with linear NCOA3 mRNA, circ_0001165 expression was little affected by RNase R digestion and actinomycin D treatment, indicating its high stability (Figs. 1D-1G). So, these data indicated an up-regulation and stable structure of circ_0001165 in PCa tissue and cells.

### 3.2. Silencing circ_0001165 inhibited PCa cell proliferation and promote apoptosis

First, two circ_0001165 knockdown vectors (sh-circ_0001165#1 and sh-circ_0001165#2) were constructed and transfected into LNCaP and DU145 cells, and knockdown efficiency was detected by qRT-PCR (Figs. 2A and 2B). MTT assay showed that sh-circ_0001165#1 and sh-circ_0001165#2 significantly reduced the cell viability of LNCaP and DU145 (Figs. 2C and 2D). EdU positive cell rate of sh-circ_0001165#1 and sh-circ_0001165#2 interfered LNCaP and DU145 cells were consistently lowered than control group cells (Fig. 2E), suggesting that silencing circ_0001165 depression on PCa cell proliferation. Flow cytometry showed that sh-circ_0001165#1 and sh-circ_0001165#2 blocked the LNCaP and DU145 cells in the G0/G1 phase (Fig. 2F). However, flow cytometry showed that sh-circ_0001165#1 and sh-circ_0001165#2 significantly promoted LNCaP and DU145 cells apoptosis (Fig. 2G). In a word, silencing circ_0001165 inhibited PCa cell proliferation and promoted apoptosis.

### 3.3. Silencing circ_0001165 inhibited PCa cell tube formation, migration, and invasion

As shown in Fig. 3A, sh-circ_0001165#1 and sh-circ_0001165#2 significantly reduced the tube formation of LNCaP and DU145 cells. Similarly, the wound-healing assay showed that sh-circ_0001165#1 and sh-circ_0001165#2 significantly reduced the wound closure rate (Fig. 3B). And, Transwell assay found that sh-circ_0001165#1 and sh-circ_0001165#2 significantly reduced the invasion of LNCaP and DU145 cells (Fig. 3C). Molecularly, epithelial-mesenchymal transition-related proteins expression was examined, the results showed that sh-circ_0001165#1 and

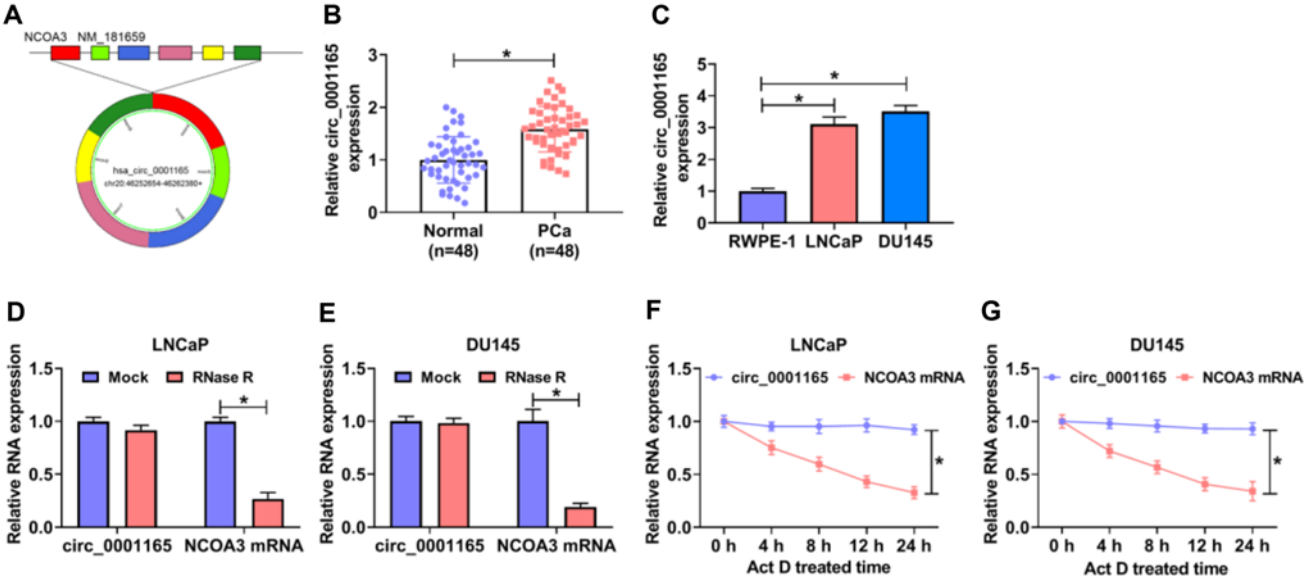


**Fig. 1.** Circ_0001165 was upregulated in prostate cancer (PCa) tissues and cell lines. (A) The structure of circ_0001165. (B, C) The expression of circ_0001165 in PCa tissues (n = 48) and cells was tested by quantitative real-time polymerase chain reaction (qRT-PCR). (D, E) RNase R degradation was used to detect the stability of circ_0001165. (F, G) The relative RNA level of circ_0001165 and NCOA3 in LNCaP and DU145 cells were analyzed by qRT-PCR after actinomycin D (Act D) treatment. *$p < 0.05$.

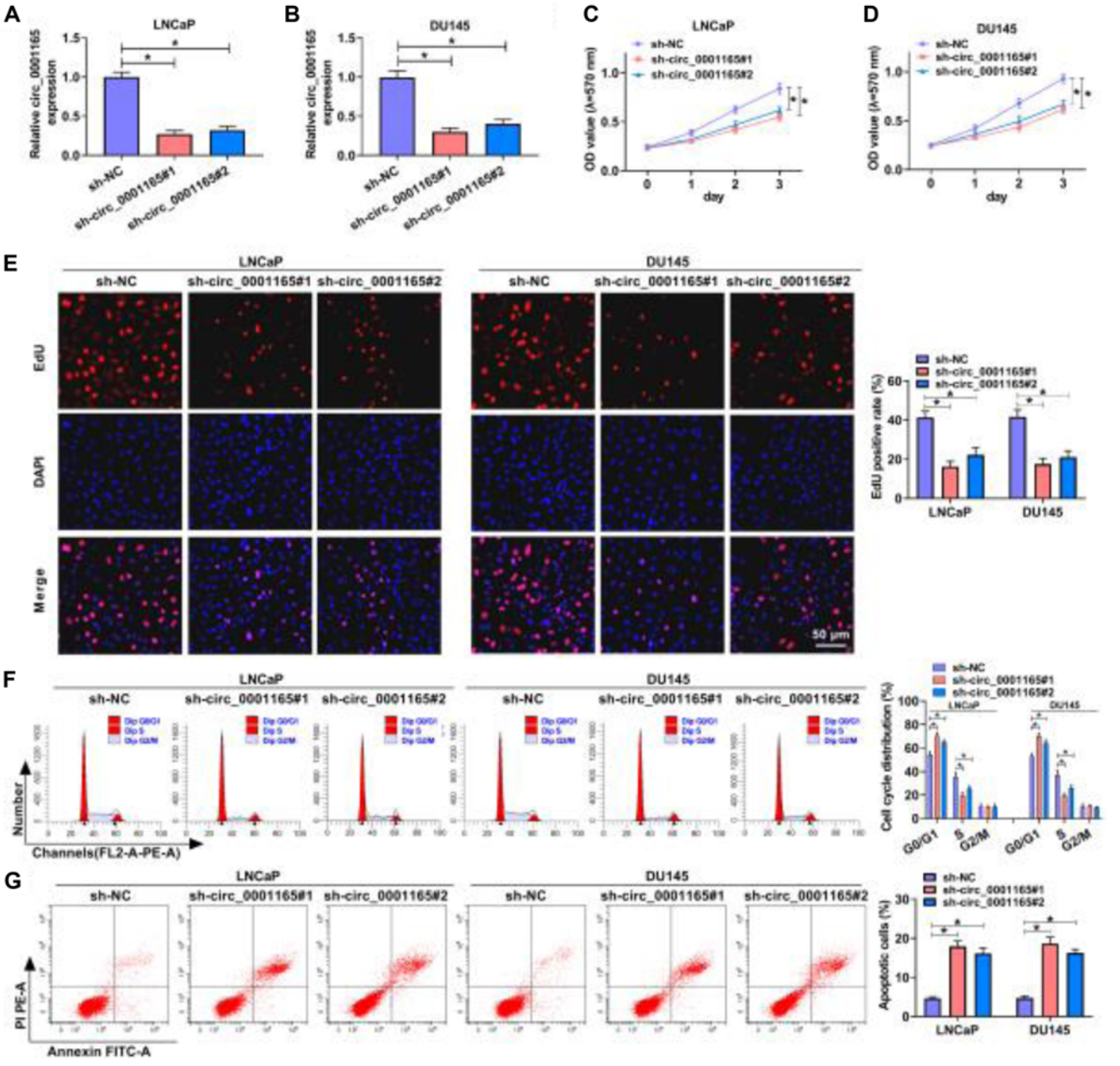


**Fig. 2.** Silencing circ_0001165 can inhibit the proliferation and promote apoptosis of prostate cancer cells. (A, B) The expression level of circ_0001165 was determined by qRT-PCR in transfected LNCaP and DU145 cells. (C, D) MTT was used to detect cell viability. (E) EdU proliferation assay was performed in transfected LNCaP and DU145 cells. (F) Cell cycle was measured by flow cytometry. (G) Cell apoptosis was detected by flow cytometry. qRT-PCR: quantitative real-time polymerase chain reaction, MTT: 3-(4, 5-dimethylthiazol-2-yl)-2, 5-diphenyltetrazolium Bromide, EdU: 5-ethynyl-2'-deoxyuridine, DAPI: 4',6-diamidino-2-phenylindole, FITC: fluorescein isothiocyanate, PI: propidium iodide. *$p < 0.05$.

sh-circ_0001165#2 significantly reduced the expression of Snail1 and Slug (Figs. 3D and 3E). In a word, knockdown of circ_0001165 suppressed PCa cell malignant behavior.

### 3.4. Circ_0001165 targeted miR-654-3p

As shown in Fig. 4A, Starbase (https://starbase.sysu.edu.cn/agoClipRNA.php?source=mRNA) and circInteractome (https://circinteractome.nia.nih.gov/mirna_target_sites.html) jointly predicted that 6 miRNAs were targeted by circ_0001165. And the over-expression efficiency of circ_0001165 was detected by qRT-PCR (Fig. 4B). Next, after circ_0001165 was transfected, the expression of six miRNAs was detected by qRT-PCR, and the results showed that the expression effect of miR-654-3p was reduced to the

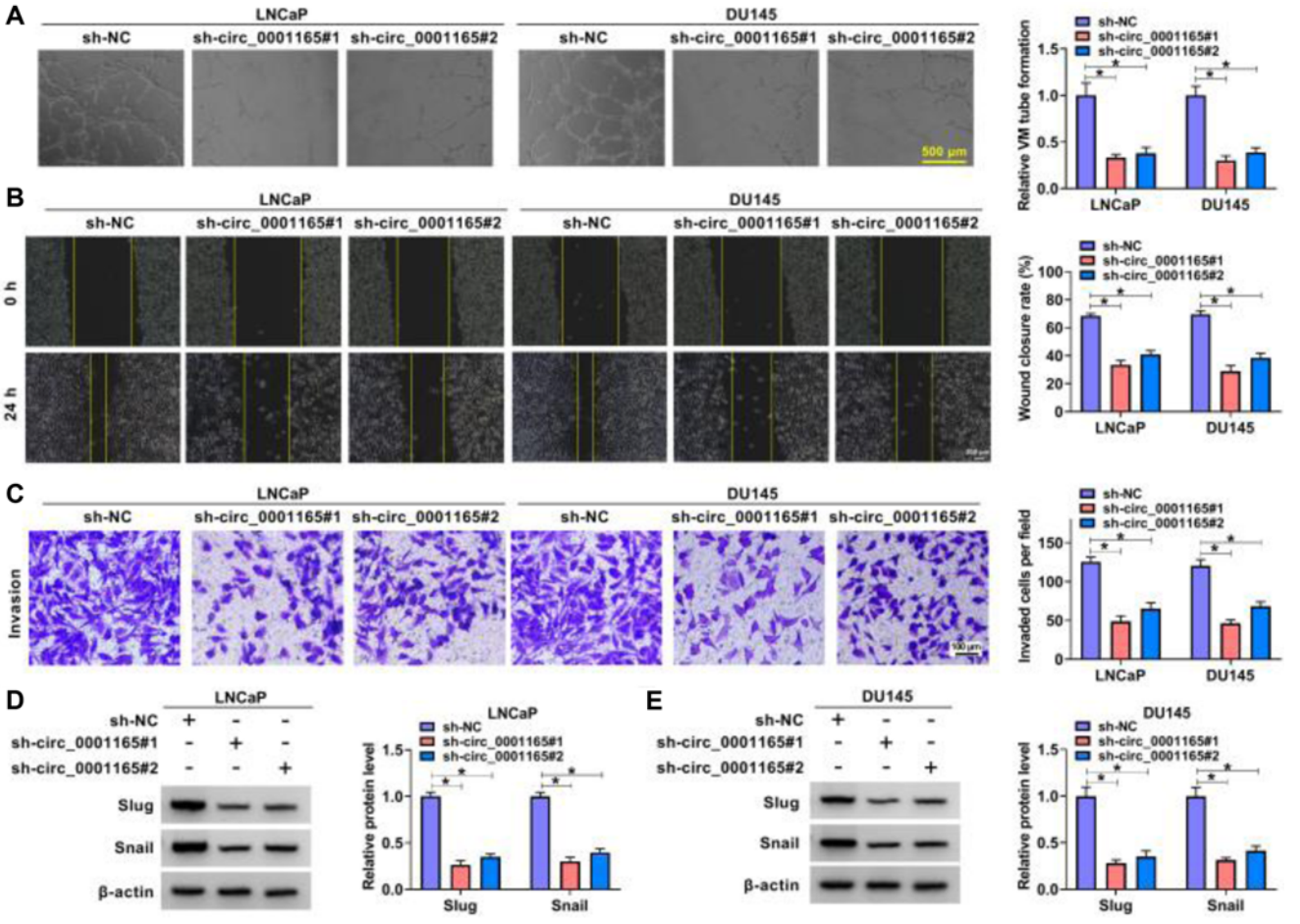


**Fig. 3.** Silencing circ_0001165 inhibits tube formation and metastasis of prostate cancer cells. (A) Tube formation assay was used to detect the relative number of branches in transfected LNCaP and DU145. (B) Wound-healing assay was used to examine the wound closure rate. (C) The role of circ_0001165 knockdown on cell invasion was monitored by Transwell assay. (D, E) The expression level of Snail and Slug was determined by Western blot. *$p < 0.05$.

greatest extent (Figs. 4C and 4D). Therefore, the regulatory relationship between circ_0001165 and miR-654-3p was further explored. Fig. 4E showed the binding site of circ_0001165 and miR-654-3p. And Fig. 4F showed the overexpression efficiency of miR-654-3p in HEK293T cell was detected by qRT-PCR. Dual-luciferase reporter assay results showed that in HEK293T cell, the combined transfection of miR-654-3p and circ_0001165-WT significantly inhibited luciferase activity, while the combined transfection of miR-654-3p and circ_0001165-MUT showed no significant change (Fig. 4G). RIP detection further confirmed the direct interaction between miR-654-3p and circ_0001165 in LNCaP and DU145 cells (Figs. 4H and 4I). qRT-PCR detected the low expression of miR-654-3p in PCa cancer cell lines and tissues (Figs. 4J and 4K). And Pearson's correlation analysis results showed that circ_0001165 was negatively correlated with miR-654-3p (Fig. 4L). In general, circ_0001165 can sponge miR-654-3p.

### 3.5. Anti-miR-654-3p restored the effect of sh-circ_0001165#1 on prostate cancer cells

In order to verify the effect of miR-654-3p on the function of circ_0001165, we set up a recovery experiment. First, the transfection efficiency of anti-miR-654-3p in LNCaP and DU145 cells was detected by qRT-PCR (Fig. 5A). Then, qRT-PCR detection revealed that sh-circ_0001165#1 up-regulated the expression of miR-654-3p, while co-transfection of anti-miR-654-3p could restore the expression level of miR-654-3p (Fig. 5B). The results of MTT assay showed that co-transfection of anti-miR-654-3p could up-regulate the cell viability reduced by sh-circ_0001165#1 (Figs. 5C and 5D). And the EdU proliferation assay showed that co-transfection of anti-miR-654-3p restored the percentage of positive cells down-regulated by knockdown of circ_0001165 (Fig. 5E). Flow cytometry showed that sh-circ_0001165#1 increased the number of LNCaP and DU145 cells in G0/G1 phase and significantly reduced the

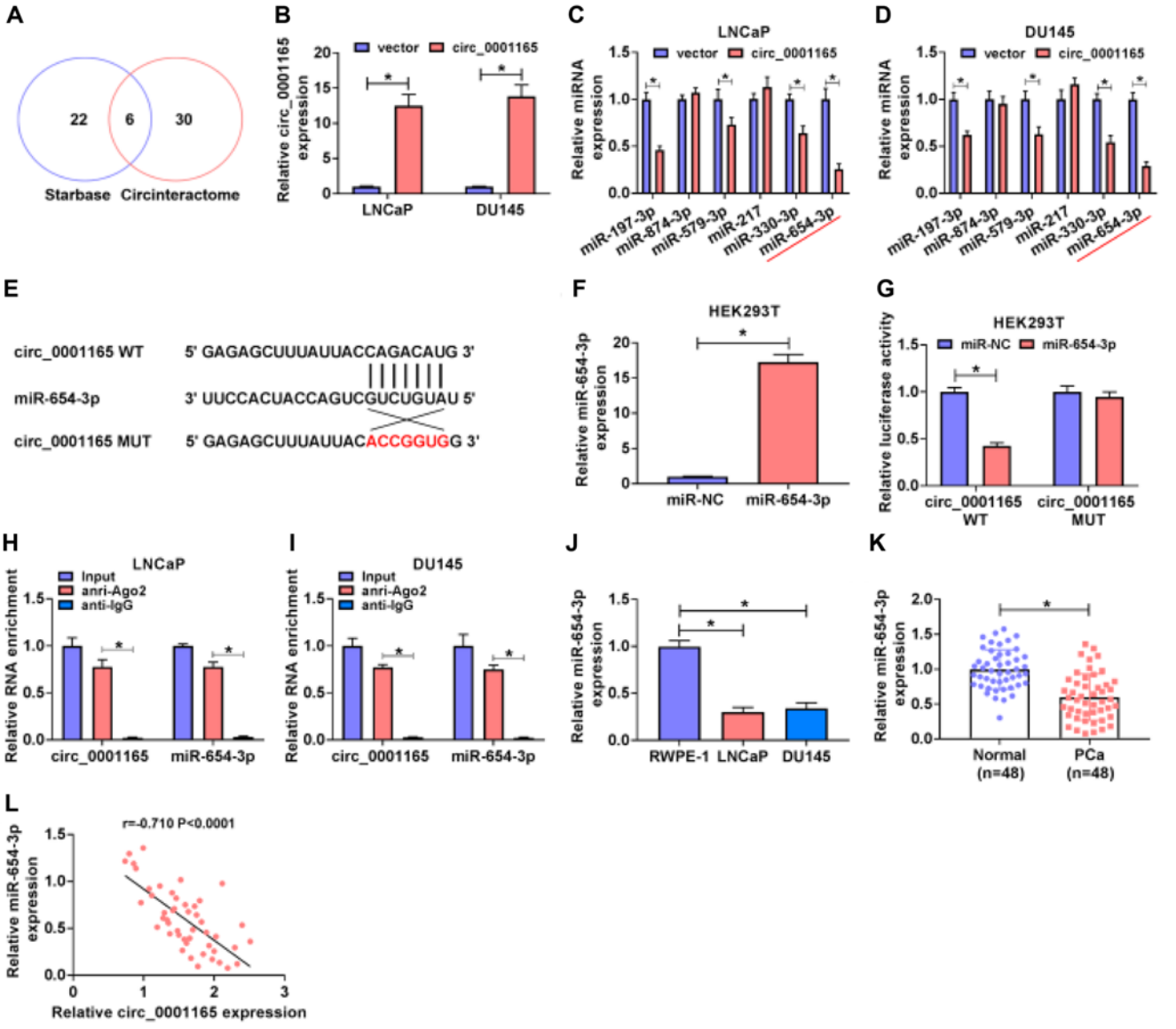


**Fig. 4.** Circ_0001165 functions as a sponge of miR-654-3p. (A) The targeting of circ_0001165 was predicted with Circinteractome and Starbase. (B) The expression of circ_0001165 in prostate cancer (PCa) cells was tested by quantitative real-time polymerase chain reaction (qRT-PCR). (C, D) The expression of six microRNAs (miRNAs) in PCa cells was detected by qRT-PCR. (E) The complementary sequences between miR-654-3p and circ_0001165 were shown. (F) The expression of miR-654-3p in HEK293T cells was tested by qRT-PCR. (G) Dual-luciferase reporter assays were performed to confirm the association between miR-654-3p and circ_0001165. (H, I) RNA immunoprecipitation assay were performed to measure the interaction between miR-654-3p and circ_0001165. (J, K) The expression of miR-654-3p in PCa tissues (n = 48) and cells was tested by qRT-PCR. (L) Pearson's correlation analysis. *p < 0.05.

number of cells in S phase, while anti-miR-654-3p restored the cell cycle to normal (Figs. 5F and 5G). And flow cytometry showed that sh-circ_0001165#1 increased the apoptosis rate of LNCaP and DU145 cells, while anti-miR-654-3p decreased the apoptosis rate (Fig. 5H). Tube formation assay also showed that anti-miR-654-3p could regulate the decrease of relative vasculogenic mimicry (VM) tube formation caused by sh-circ_0001165#1 (Fig. 5I). Mechanically, wound-healing assay found that anti-miR-654-3p could improve the wound closure rate reduced by sh-circ_0001165#1 (Fig. 5J). Similarly, Transwell found that sh-circ_0001165#1 could decrease number of invasion, while anti-miR-654-3p up-regulated it (Fig. 5K). Lastly, Western blot results showed that sh-circ_0001165#1 could down-regulation of Snail1 and Slug proteins, while co-transfection of anti-miR-654-3p reversed it (Fig. 5L). In general, miR-654-3p inhibitors restored cell malignant behavior reduced by sh-circ_0001165#1.

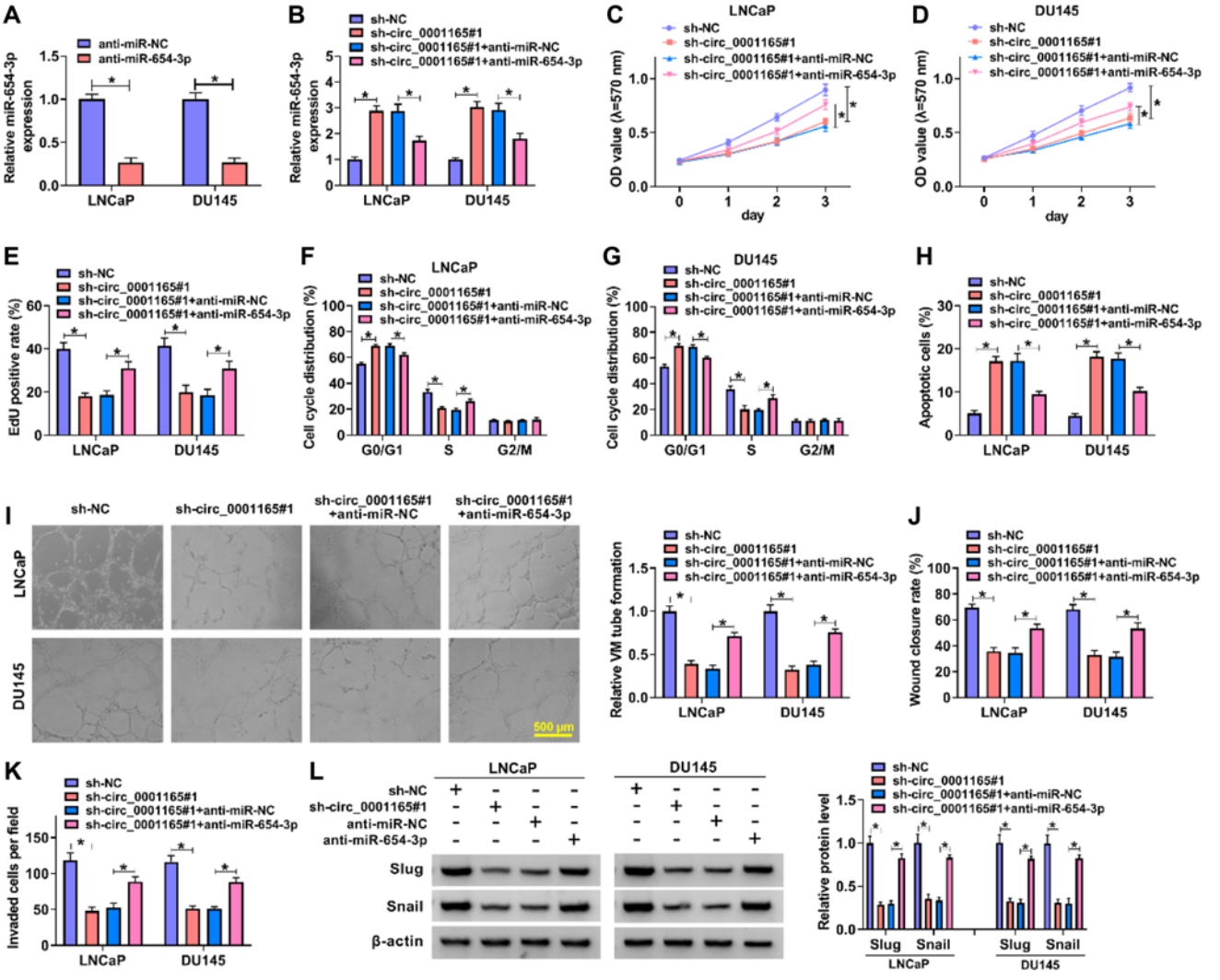


**Fig. 5.** Circ_0001165 regulate the malignant behavior by targeting miR-654-3p in prostate cancer cells. (A, B) qRT-PCR detected the expression of miR-654-3p in transfected LNCaP and DU145 cells. (C, D) MTT was used to detect cell viability. (E) EdU proliferation assay was performed in transfected LNCaP and DU145 cells. (F, G) Cell cycle was measured by flow cytometry. (H) Cell apoptosis was detected by flow cytometry. (I) Tube formation assay was used to detect the relative number of branches in transfected LNCaP and DU145. (J) Wound-healing assay was used to examine the wound closure rate. (K) Cell invasion was monitored by Transwell assay. (L) The expression level of Snail and Slug was determined by Western blot. qRT-PCR: quantitative real-time polymerase chain reaction, MTT: 3-(4, 5-dimethylthiazol-2-yl)-2, 5-diphenyltetrazolium Bromide, EdU: 5-ethynyl-2'-deoxyuridine, OD: optical density. *$p < 0.05$.

### 3.6. DDAH1 was a direct target of miR-654-3p

Using Targetscan software (http://www.targetscan.org/vert_72/) forecast the binding sites between DDAH1 3'UTR and miR-654-3p (Fig. 6A). The overexpression of miR-654-3p inhibited the luciferase activity of the DDAH1 3'UTR-WT, but did not affect the luciferase activity of the DDAH1 3'UTR-MUT (Fig. 6B). Western blot showed that the expression level of DDAH1 was significantly increased in PCa cancer cell lines and tissues (Figs. 6C-6E). And Pearson's correlation analysis results showed that DDAH1 was negatively correlated with miR-654-3p, and DDAH1 was positively correlated with circ_0001165 (Figs. 6F and 6G). Next, qRT-PCR detected the miR-654-3p overexpression efficiency (Fig. 6H). Western blot detected the DDAH1 overexpression efficiency (Fig. 6I). And, the expression of DDAH1 was detected by Western blot to verify the regulatory relationship between miR-654-3p and DDAH1, the results show that, overexpression of miR-654-3p inhibited the expression of DDAH1 in PCa cells, while co-transfection with DDAH1 could partially reverse it (Fig. 6J). Finally, sh-circ_0001165#1 inhibited the expression of DDAH1 in PCa cells, while co-transfection with anti-miR-654-3p could partially reversed it (Fig. 6K). In general, DDAH1 was a direct target of miR-654-3p.

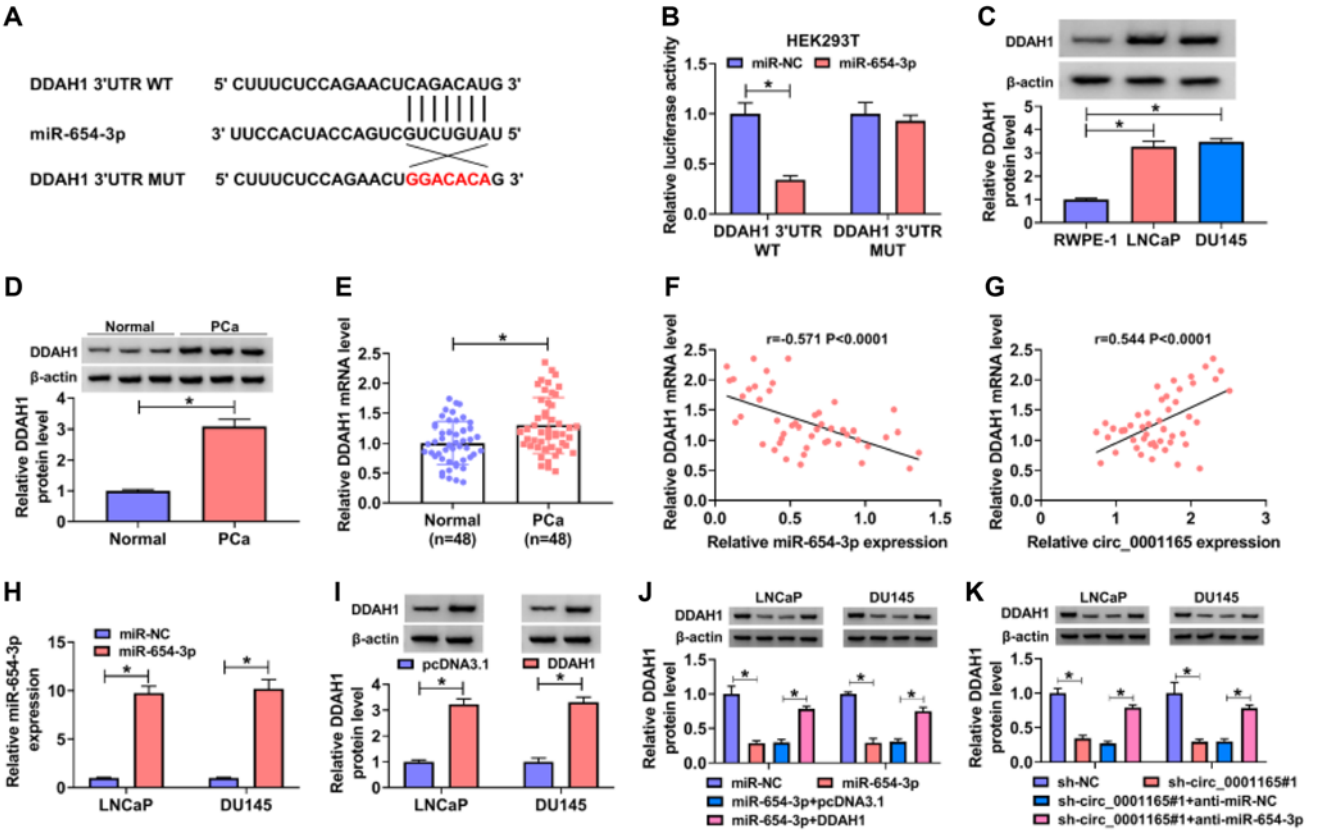


**Fig. 6.** Dimethylarginine dimethylaminohydrolase 1 (DDAH1) is the direct target of miR-654-3p. (A) The complementary sequences between miR-654-3p and DDAH1 were shown. (B) Dual-luciferase reporter assays were performed to confirm the association between miR-654-3p and DDAH1 3'UTR. (C, D) Western blot assay examined the protein level of DDAH1 in prostate cancer (PCa) tissues (n = 48) and cells. (E) Quantitative real-time polymerase chain reaction (qRT-PCR) detected the expression of DDAH1 in PCa tissues (n = 48). (F, G) Pearson's correlation analysis. (H) The expression of miR-654-3p examined by qRT-PCR. (I-K) Western blot was used to examine the expression of DDAH1. *p < 0.05.

### 3.7. DDAH1 restored the effect of miR-654-3p on prostate cancer cells

In order to verify the effect of DDAH1 on the function of miR-654-3p, we set up a recovery experiment. The results of MTT assay showed that co-transfection of DDAH1 could up-regulate the cell viability reduced by miR-654-3p (Figs. 7A and 7B). And the EdU proliferation assay showed that co-transfection of DDAH1 restored the percentage of positive cells down-regulated by miR-654-3p (Fig. 7C). Flow cytometry showed that miR-654-3p increased the number of LNCaP and DU145 cells in G0/G1 phase and significantly reduced the number of cells in S phase, while DDAH1 restored the cell cycle to normal (Figs. 7D and 7E). And flow cytometry showed that miR-654-3p increased the apoptosis rate of LNCaP and DU145 cells, while DDAH1 decreased the apoptosis rate (Fig. 7F). Tube formation assay also showed that DDAH1 could regulate the decrease of relative VM tube formation caused by miR-654-3p (Figs. 7G and 7H). Mechanically, wound-healing assay found that DDAH1 could improve the wound closure rate reduced by miR-654-3p (Fig. 7I). Similarly, Transwell found that miR-654-3p could decrease number of invasion, while DDAH1 up-regulated it (Fig. 7J). Similarly, Western blot results showed that miR-654-3p down-regulation of Snail1 and Slug proteins, while co-transfection of DDAH1 reverse it (Figs. 7K-7N). In general, DDAH1 restored cell malignant behavior reduced by miR-654-3p.

### 3.8. Circ_0001165 knockdown inhibited tumor growth *in vivo*

In order to better investigate the effect of circ_0001165 on PCa, we constructed a xenotransplantation model of hepatocellular carcinoma. By recording and observing tumor volume (Fig. 8A) and tumor weight (Figs. 8B and 8C), we found that knocking down circ_0001165 significantly inhibited tumor growth. Then, qRT-PCR detection results showed that after circ_0001165 knockdown, the expressions

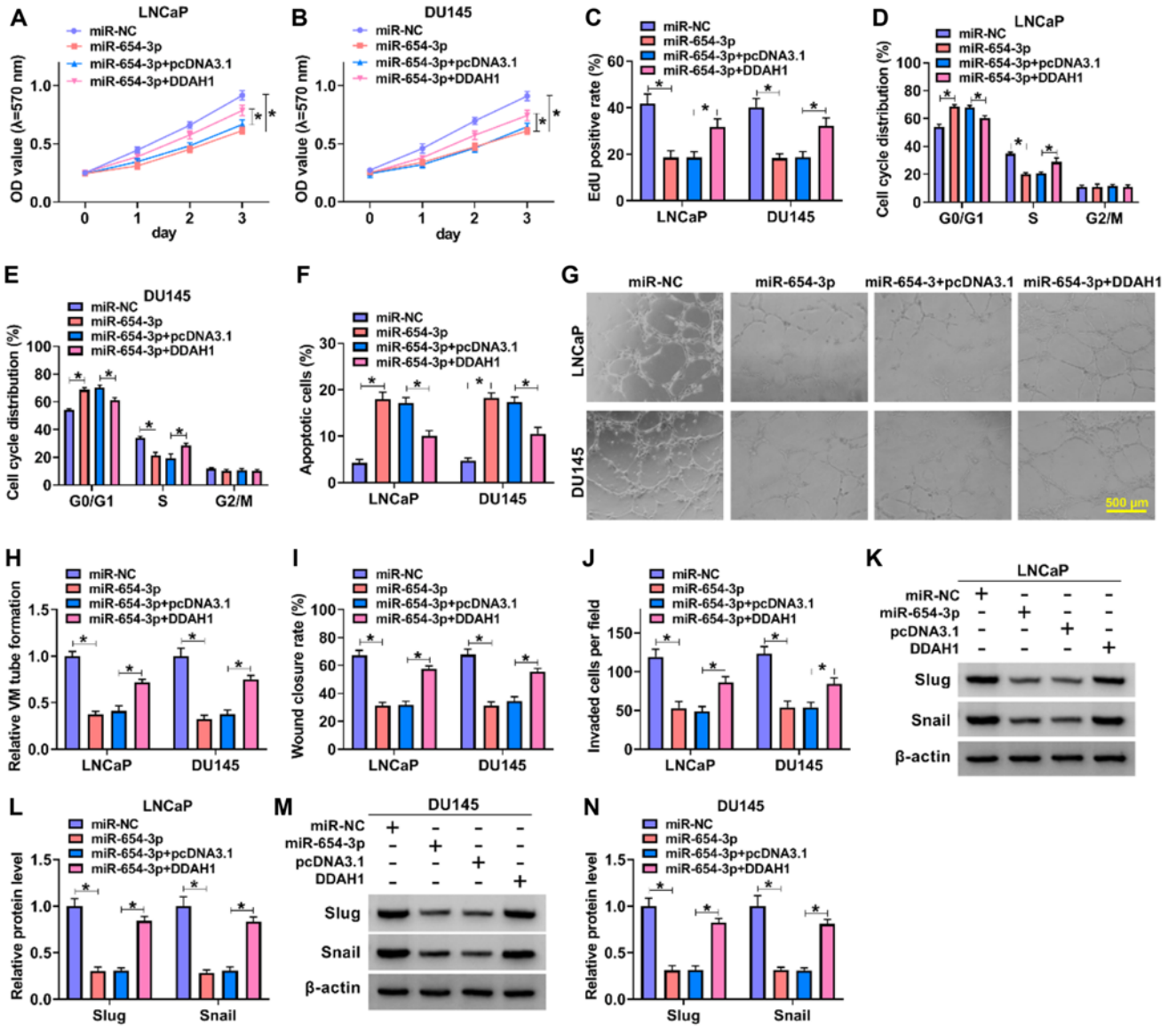


**Fig. 7.** Circ_0001165 regulate the proliferation, migration, and invasion by targeting DDAH1 in prostate cancer cells. (A, B) MTT was used to detect cell viability. (C) EdU proliferation assay was performed in transfected LNCaP and DU145 cells. (D, E) Cell cycle was measured by flow cytometry. (F) Cell apoptosis was detected by flow cytometry. (G, H) Tube formation assay was used to detect the relative number of branches in transfected LNCaP and DU145. (I) Wound-healing assay was used to examine the wound closure rate. (J) Cell invasion was monitored by Transwell assay. (K-N) The expression level of Snail and Slug was determined by Western blot. DDAH1: dimethylarginine dimethylaminohydrolase 1, MTT: 3-(4, 5-dimethylthiazol-2-yl)-2, 5-diphenyltetrazolium Bromide, EdU: 5-ethynyl-2'-deoxyuridine, OD: optical density. *p < 0.05.

of circ_0001165 (Fig. 8D) in the tumor were significantly decreased, and the expressions of miR-654-3p were significantly increased (Fig. 8E). Similarly, Western blot analysis also confirmed that sh-circ_0001165 significantly reduced DDAH1 protein levels (Fig. 8F). Finally, IHC results also showed that knocking down circ_0001165 significantly reduced the positive rate of Ki67 (Fig. 8G). In conclusion, down-regulation of circ_0001165 reduced the tumor development of PCa.

## 4. Discussion

It is well known that circRNAs, as ceRNAs through sponge miRNAs, were involved in the pathogenesis of various human diseases, including cancer [25]. Several studies suggested that circRNAs have ceRNAs activity in the development of PCa. However, studied the exact role of circRNA in the progression of PCa through the ceRNAs network has been a challenge. Here, we demonstrated for

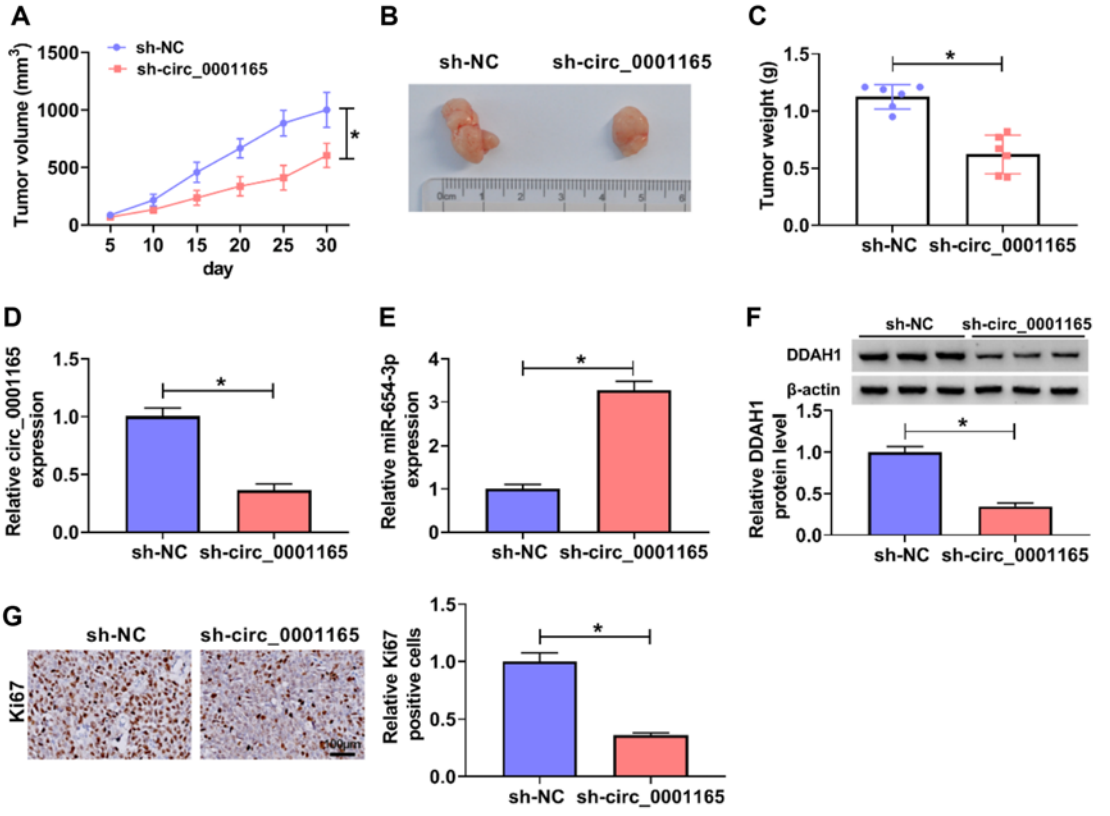


**Fig. 8.** Circ_0001165 knockdown inhibited tumor growth *in vivo*. (A-C) Tumor volume and weight after circ_0001165 knockdown *in vivo*. (D, E) Relative expression levels of circ_0001165 and miR-654-3p in xenografts were detected by qRT-PCR. (F) Western blot examined the expression of DDAH1. (G) The positive rate of Ki67 was analyzed by IHC. qRT-PCR: quantitative real-time polymerase chain reaction, DDAH1: dimethylarginine dimethylaminohydrolase 1, IHC: immunohistochemical. *p < 0.05.

the first time the role of circ_0001165 as a novel regulator of PCa cell functional characteristics by regulating the miR-654-3p/DDAH1 axis.

Our results showed that circ_0001165 was highly-expressed in PCa tissues and cells, this result was consistent with previous findings [12]. In this study, the role of circ_0001165 in PCa cell lines LNCaP and DU145 was investigated by functional cell assay. The results showed that silence circ_0001165 inhibited the cell malignant behavior of LNCaP and DU145 cells, and promoted cell apoptosis. Current studies have found that angiogenesis was one of the hallmarks of tumors, which promoted the growth and development of tumors [26]. Using an angiogenesis assay, we demonstrated for the first time that silencing circ_0001165 inhibited angiogenesis in PCa cells. This suggested that tumor angiogenesis inhibition from knocking down circ_0001165 can be used as a therapeutic strategy for the treatment of PCa. Similarly, circ_0001165 silencing also inhibits PCa tumor growth *in vivo*. It is worth mentioning that our subsequent study showed that circ_0001165 played a role in PCa cells by regulating the expression of miR-654-3p.

According to the above results, we understood the mechanism of circ_0001165 in PCa. Since circRNAs could adsorb other miRNAs and play a regulatory role, then, we found that miR-654-3p was a target gene of circ_0001165. And our results confirmed that miR-654-3p was an effective tumor inhibitor in PCa, which was consistent with the results of previous studies [27]. A series of complement experiments were designed to explore whether it can regulate PCa. The results showed that miR-654-3p inhibitor could restore the malignant behavior of PCa cells inhibited by silence circ_0001165. We also found that DDAH1 was a direct and functional target of miR-654-3p. Consistent with the results of Reddy *et al.* [24], we found that DDAH1 was significantly overexpressed in PCa. More importantly, we show that the ceRNA activity of circ_0001165 regulated DDAH1 expression through sponge miR-654-3p.

In summary, circ_0001165 was established here as a new regulator of PCa progression. We discovered a novel circ_0001165/miR-654-3p/DDAH1 regulatory network in the development of PCa. Therefore, the circ_0001165 inhibitor appeared to be a promising candidate for the development of new antitumor therapies for PCa.

## Ethical Statements

The authors declare that they have no conflicts of interest. The design of this protocol follows the tenets of the Declaration of Helsinki, approved by the Ethics Committee of Wuhan Hankou Hospital.

## Electronic Supplementary Material (ESM)

The online version of this article (doi: 10.1007/s12257-021-0229-4) contains supplementary material, which is available to authorized users.

## References


1. Xin, L. (2019) Cells of origin for prostate cancer. *Adv. Exp. Med. Biol.* 1210: 67-86.
2. Merriel, S. W. D., G. Funston, and W. Hamilton (2018) Prostate cancer in primary care. *Adv. Ther.* 35: 1285-1294.
3. Abrams, D. I. (2018) An integrative approach to prostate cancer. *J. Altern. Complement. Med.* 24: 872-880.
4. Zhou, C. K., D. P. Check, J. Lortet-Tieulent, M. Laversanne, A. Jemal, J. Ferlay, F. Bray, M. B. Cook, and S. S. Devesa (2016) Prostate cancer incidence in 43 populations worldwide: an analysis of time trends overall and by age group. *Int. J. Cancer* 138: 1388-1400.
5. Siegel, R. L., K. D. Miller, and A. Jemal (2016) Cancer statistics, 2016. *CA Cancer J. Clin.* 66: 7-30.
6. Sartor, O. and J. S. de Bono (2018) Metastatic prostate cancer. *N. Engl. J. Med.* 378: 645-657.
7. Chen, L. L. and L. Yang (2015) Regulation of circRNA biogenesis. *RNA Biol.* 12: 381-388.
8. Liu, J., T. Liu, X. Wang, and A. He (2017) Circles reshaping the RNA world: from waste to treasure. *Mol. Cancer.* 16: 58.
9. Ding, T., Y. Zhu, H. Jin, P. Zhang, J. Guo, and J. Zheng (2021) Circular RNA circ_0057558 controls prostate cancer cell proliferation through regulating miR-206/USP33/c-Myc axis. *Front. Cell Dev. Biol.* 9: 644397.
10. Li, X., B. Azhati, W. Wang, M. Rexiati, C. Xing, and Y. Wang (2021) Circular RNA UBAP2 promotes the proliferation of prostate cancer cells via the miR-1244/MAP3K2 axis. *Oncol. Lett.* 21: 486.
11. Mao, Y., W. Li, B. Hua, X. Gu, W. Pan, Q. Chen, B. Xu, C. Lu, and Z. Wang (2021) Circular RNA_PDHX promotes the proliferation and invasion of prostate cancer by sponging MiR-378a-3p. *Front. Cell Dev. Biol.* 8: 602707.
12. Yan, Z., Y. Xiao, Y. Chen, and G. Luo (2020) Screening and identification of epithelial-to-mesenchymal transition-related circRNA and miRNA in prostate cancer. *Pathol. Res. Pract.* 216: 152784.
13. Hansen, T. B., T. I. Jensen, B. H. Clausen, J. B. Bramsen, B. Finsen, C. K. Damgaard, and J. Kjems (2013) Natural RNA circles function as efficient microRNA sponges. *Nature.* 495: 384-388.
14. Gregory, R. I. and R. Shiekhattar (2005) MicroRNA biogenesis and cancer. *Cancer Res.* 65: 3509-3512.
15. Macfarlane, L. A. and P. R. Murphy (2010) MicroRNA: biogenesis, function and role in cancer. *Curr. Genomics*. 11: 537-561.
16. Pu, J. T., Z. Hu, D. G. Zhang, T. Zhang, K. M. He, and T. Y. Dai (2020) MiR-654-3p suppresses non-small cell lung cancer tumourigenesis by inhibiting PLK4. *Onco Targets Ther.* 13: 7997-8008.
17. Yang, J., Z. Zhang, S. Chen, W. Dou, R. Xie, and J. Gao (2020) miR-654-3p predicts the prognosis of hepatocellular carcinoma and inhibits the proliferation, migration, and invasion of cancer cells. *Cancer Biomark.* 28: 73-79.
18. Formosa, A., E. K. Markert, A. M. Lena, D. Italiano, E. Finazzi-Agro', A. J. Levine, S. Bernardini, A. V. Garabadgiu, G. Melino, and E. Candi (2014) MicroRNAs, miR-154, miR-299-5p, miR-376a, miR-376c, miR-377, miR-381, miR-487b, miR-485-3p, miR-495 and miR-654-3p, mapped to the 14q32.31 locus, regulate proliferation, apoptosis, migration and invasion in metastatic prostate cancer cells. *Oncogene*. 33: 5173-5182.
19. Frey, D., O. Braun, C. Briand, M. Vasák, and M. G. Grütter (2006) Structure of the mammalian NOS regulator dimethylarginine dimethylaminohydrolase: a basis for the design of specific inhibitors. *Structure.* 14: 901-911.
20. Leiper, J. M., J. Santa Maria, A. Chubb, R. J. MacAllister, I. G. Charles, G. S. Whitley, and P. Vallance (1999) Identification of two human dimethylarginine dimethylaminohydrolases with distinct tissue distributions and homology with microbial arginine deiminases. *Biochem. J.* 343: 209-214.
21. Dayal, S., R. N. Rodionov, E. Arning, T. Bottiglieri, M. Kimoto, D. J. Murry, J. P. Cooke, F. M. Faraci, and S. R. Lentz (2008) Tissue-specific downregulation of dimethylarginine dimethylaminohydrolase in hyperhomocysteinemia. *Am. J. Physiol. Heart Circ. Physiol.* 295: H816-H825.
22. Ye, J., J. Xu, Y. Li, Q. Huang, J. Huang, J. Wang, W. Zhong, X. Lin, W. Chen, and X. Lin (2017) DDAH1 mediates gastric cancer cell invasion and metastasis via Wnt/β-catenin signaling pathway. *Mol. Oncol.* 11: 1208-1224.
23. Ding, X., J. Zheng, and M. Cao (2021) Circ_0004771 accelerates cell carcinogenic phenotypes via suppressing miR-1253-mediated DDAH1 inhibition in breast cancer. *Cancer Manag. Res.* 13: 1-11.
24. Reddy, K. R. K., C. Dasari, D. Duscharla, B. Supriya, N. S. Ram, M. V. Surekha, J. M. Kumar, and R. Ummanni (2018) Dimethylarginine dimethylaminohydrolase-1 (DDAH1) is frequently upregulated in prostate cancer, and its overexpression conveys tumor growth and angiogenesis by metabolizing asymmetric dimethylarginine (ADMA). *Angiogenesis.* 21: 79-94.
25. Arnaiz, E., C. Sole, L. Manterola, L. Iparraguirre, D. Otaegui, and C. H. Lawrie (2019) CircRNAs and cancer: biomarkers and master regulators. *Semin. Cancer Biol.* 58: 90-99.
26. Ricciuti, B., J. Foglietta, V. Bianconi, A. Sahebkar, and M. Pirro (2019) Enzymes involved in tumor-driven angiogenesis: a valuable target for anticancer therapy. *Semin. Cancer Biol.* 56: 87-99.
27. Yu, Q., P. Li, M. Weng, S. Wu, Y. Zhang, X. Chen, Q. Zhang, G. Shen, X. Ding, and S. Fu (2018) Nano-vesicles are a potential tool to monitor therapeutic efficacy of carbon ion radiotherapy in prostate cancer. *J. Biomed. Nanotechnol.* 14: 168-178.